

# Isolation and in vitro characterisation of dental pulp stem cells from natal teeth

Erdal Karaöz · Burcu Nur Doğan · Ayça Aksoy · Gülçin Gacar · Serap Akyüz · Selda Ayhan · Zehra Seda Genç · Sinan Yürüker · Gökhan Duruksu · Pınar Çetinalp Demircan · Ayla Eker Sarıboyacı

Accepted: 23 September 2009 / Published online: 9 October 2009  
© Springer-Verlag 2009

**Abstract** Dental pulp stem cells were primarily derived from the pulp tissues of exfoliated deciduous teeth, primary incisors and permanent third molar teeth. The aim of this study was to isolate and extensively characterise SCs derived from human natal dental pulp (hNDP). For characterisation, proliferation capacity, phenotypic properties, ultrastructural and differentiation characteristics and gene expression profiles were utilised. A comparison was done between the properties of NDP-SCs and the properties of mesenchymal stem cells (MSCs) from bone marrow (BM) of the human. Stem cells isolated from hNDP and hBM were analysed by flow cytometry, reverse transcriptase-PCR, Real Time-PCR, and immunocytochemistry. Both cell lines were directionally differentiated towards adipogenic, osteogenic chondrogenic, myogenic and neurogenic lineages. hNDP-SCs and hBM-MSCs expressed CD13, CD44, CD90, CD146 and CD166, but not CD3, CD8, CD11b, CD14, CD15, CD19, CD33, CD34, CD45, CD117, and HLA-DR. Ultrastructural characteristics of hNDP-SCs showed more developed and metabolically active cells. hNDP-SCs and hBM-MSCs expressed some adipogenic

(leptin, adipophilin and PPAR $\gamma$ ), myogenic (desmin, myogenin, myosinIIa, and  $\alpha$ -SMA), neurogenic ( $\gamma$ -enolase, MAP2a,b, c-fos, nestin, NF-H, NF-L, GFAP and betaIII tubulin), osteogenic (osteonectin, osteocalcin, osteopontin, Runx-2, and type I collagen) and chondrogenic (type II collagen, SOX9) markers without any stimulation towards differentiation under basal conditions. Embryonic stem cell markers Oct4, Rex-1, FoxD-3, Sox2, and Nanog were also identified. The differentiation potential of hNDP-SCs and hBM-MSCs to adipogenic, osteogenic, chondrogenic, myogenic and neurogenic was shown. This report described the first successful isolation and characterisation of hNDP-SCs.

**Keywords** Human · Dental pulp · Natal teeth · Bone marrow · Mesenchymal stem cell · In vitro · Characterisation

## Introduction

Due to their similar characteristics with other mesenchymal stem cells (MSCs) and the relative ease at which they can be obtained and propagated, mesenchymal stem cells derived from dental pulp have become increasingly popular to study. Detailed in vivo and in vitro studies were previously carried out to examine the proliferation and differentiation capacity of MSCs derived from dental pulp. The first report in this area, published by Gronthos et al. (2000), revealed that stem cells isolated from the dental pulp of wisdom teeth, formed dentin/pulp-like structures both in vivo and in vitro. Later, the same group (2003) was able to produce ectomesenchymal stem cells from exfoliated deciduous teeth (Miura et al. 2003).

In other studies, researchers induced the differentiation of stem cells isolated from dental pulp (DPSCs) derived

E. Karaöz (✉) · A. Aksoy · G. Gacar · S. Ayhan · Z. S. Genç · G. Duruksu · P. Ç. Demircan · A. E. Sarıboyacı  
Stem Cell and Gene Therapy Research and Applied Center,  
Kocaeli University, 41380 Kocaeli, Turkey  
e-mail: ekaraoz@hotmail.com

B. N. Doğan · S. Akyüz  
Department of Pedodontics, Faculty of Dentistry,  
University of Marmara, 34100 Istanbul, Turkey

S. Yürüker  
Department of Histology and Embryology,  
Faculty of Medicine, University of Hacettepe,  
06100 Ankara, Turkey

from deciduous teeth or wisdom teeth into various cell types (Nosrat et al. 2001; Shi et al. 2001; Gronthos et al. 2002; Laino et al. 2005; Ikeda et al. 2006; d'Aquino et al. 2007; Struys et al. 2007; Huang et al. 2008). Overall, experiments revealed that stem cells and/or precursor cells derived from dental pulp can differentiate into dentin-producer odontoblasts, osteoblasts, adipocytes, skeletal and/or smooth muscle cells, endothelial cells, neural cells and elastic cartilage cells both in vivo and in vitro (Arthur et al. 2008; d'Aquino et al. 2007; Gandia et al. 2008; Gronthos et al. 2000, 2002; Huang et al. 2008; Iohara et al. 2004; Jo et al. 2007; Kerkis et al. 2006; Laino et al. 2005; Miura et al. 2003; Nosrat et al. 2001; Otaki et al. 2007; Papaccio et al. 2006; Yu et al. 2007; Zhang et al. 2006a, b).

Huang et al. (2008) demonstrated the feasibility of deriving DPSCs from tissue that is usually discarded such as supernumerary teeth. The presence of teeth in a newborn is uncommon, appearing in approximately one in every 2,000 to 3,000 live births. The majority of natal teeth are normal, primary teeth that erupted early and less than 10% of natal teeth are supernumerary. The aim of this study was to isolate and extensively characterise SCs derived from human natal dental pulp (hNDP). Furthermore, the properties of hNDP-SCs and of MSCs isolated from human bone marrow (hBM) were compared.

## Materials and methods

### Isolation and culturing of hNDP-SCs

Two vital human natal teeth were obtained from a healthy newborn female. The teeth were immersed in a physiological solution containing antibiotics to eliminate any contamination. Soon after the extraction, under sterile conditions, pliers (bone forceps) were used to fracture the dental crown into several parts and the dental pulp was uncovered. The pulp tissue was digested using collagenase type I (Sigma-Aldrich, St. Louis MO) to generate single cell suspensions. The cells were cultured in MEM-Earle (Biochrom-FG0325) containing 15% foetal bovine serum (FBS; Invitrogen/GIBCO, Grand Island, NY, USA) and 100 IU/ml penicillin-100 µg/ml streptomycin (Invitrogen/GIBCO). The cells from one tooth were seeded into two 25 cm<sup>2</sup> plastic tissue culture flasks (BD Biosciences) and incubated at 37°C in a humid atmosphere containing 5% CO<sub>2</sub> for 3 days. The stem cells were isolated based on their ability to adhere to culture plates. On the third day, red blood cells and other non-adherent cells were removed and fresh medium was added to allow further growth. The adherent cells were grown to 70% confluency and were defined as passage zero (P<sub>0</sub>) cells. Later passages were named accordingly. For passaging, the cells were washed with Ca<sup>2+</sup>-Mg<sup>2+</sup> free

phosphate-buffered saline (PBS) (Invitrogen/GIBCO) and detached by incubating with 0.25 % trypsin-EDTA solution (Invitrogen/GIBCO) for 5–10 min at 37°C. Growth medium was added to inactivate the trypsin. The cells were then centrifuged at 200×g for 10 min, resuspended in 1 ml complete medium, counted in duplicate using a Thoma chamber, and then plated in 75 cm<sup>2</sup> flasks (BD Biosciences) at a concentration of 1 × 10<sup>6</sup> cells/flask. Growth medium was replaced every 3 days over a 10–14 day period.

### Isolation and culture of hBM-MSCs

Bone marrow aspirates of 2–4 ml were taken from the iliac crest of patients (*n* = 5, age = 4–7 years) who were diagnosed with idiopathic thrombocytopenic purpura (ITP). Flow cytometry demonstrated that the individuals were actually healthy. Informed consent was received in accordance with the terms of the ethics committee of the University of Kocaeli. The bone marrow was diluted 1:3 with PBS and layered over a Ficoll-histopaque gradient (1.077 g/ml). The low-density mononuclear cells were washed twice with PBS, counted, and 1 × 10<sup>6</sup> cells/cm<sup>2</sup> were plated in culture flasks in MEM-Earle containing 15% foetal bovine serum, 100 IU/ml penicillin, and 100 µg/ml streptomycin. The cells were incubated at 37°C in a humid atmosphere containing 5% CO<sub>2</sub> for 3 days. The mesenchymal stem cells were isolated based on their ability to adhere to culture plates. On the third day, red blood cells and other non-adherent cells were removed and fresh medium was added to allow further growth. The adherent cells were grown to 70% confluency and were defined as passage zero (P<sub>0</sub>) cells. Passaging of the cells was performed as described above.

### Electron microscopy

SCs at passage three were centrifuged at 200×g for 5 min. and the pellet was fixed with 2.5% glutaraldehyde (Fluka) in 0.1 M Sorensen phosphate buffer (pH 7.2) for 24 h at 4°C. Next, the pellet was embedded in agar powder and post-fixed with 1% OsO<sub>4</sub> (Sigma-Aldrich, St. Louis, MO, USA) supplemented buffer for 1 h at room temperature. Samples were dehydrated and embedded in araldite CY212 (Sigma-Aldrich). Ultrathin sections were counterstained with lead citrate and uranyl acetate and ultrastructural observations were made using a Jeol JEM-1400 transmission electron microscope.

### Phenotype identification

#### Flow cytometry

To confirm that hNDP-SCs and hBM-MSCs maintain their phenotypic characteristics after growth in culture,

undifferentiated SCs were subjected to flow cytometry analysis. After each passage, stem cells were harvested and suspended in their own culture medium at a concentration of  $1 \times 10^6$  cells/ml. Flow cytometry was performed using a FACSCalibur (BD Biosciences, San Diego, USA). The data were analysed with Cell Quest software (BD Biosciences) and the forward and side scatter profile gated out debris and dead cells.

Immunophenotyping of hNDP-SCs and hBM-MSCs was performed with antibodies against the following human antigens: CD3 (T-cell receptor; PerCP), CD8 (Cytotoxic T-cell receptor; PE), CD10 (N-cadherin/common leucocyte lymphocytic leukaemia antigen-CALLA; PE), CD11b (Mac-1  $\alpha$ ; integrin  $\alpha_M$  chain; PE), CD13 (Aminopeptidase N/Vcadherin; PE), CD14 (Monocyte differentiation antigen/LPS receptor; FITC), CD15 (3-fucosyl-*N*-acetyl-lactosamine; PE), CD19 (PerCP-Cy5.5), CD33 (Sialic Acid-Binding Immunoglobulin-Like Lectin 3; SIGLEC3; a surface marker for very early bone marrow-derived hematopoietic stem cells; PE), CD34 (Hematopoietic Progenitor Cell Antigen; PE), CD44 (Hyaluronate/lymphocyte homing-associated cell adhesion molecule-HCAM; PE), CD45 (Protein tyrosine phosphatase, receptor type, C/ PTPRC/ leucocyte common antigen/cell marker of hematopoietic origin; FITC), CD71 (transferrin receptor, PE), CD73 (5'-nucleotidase, ecto;NT5E/integrin  $\beta_5$ ; PE), CD90 (Thy-1/Thy-1.1-FITC), CD117 (KIT or C-kit receptor/hematopoietic stem cells; PE), CD146 (melanoma cell adhesion molecule; MCAM/ a marker for endothelial cell lineage; PE), CD166 (activated leucocyte cell adhesion molecule; ALCAM/ integrin  $\alpha_3$ ; mesenchymal stem cell marker; PE) and HLA-DR (major histocompatibility complex, MHC class II, cell surface receptor; FITC). All of the antibodies were supplied by Becton Dickinson.

#### Immunohistochemistry

To identify cell characteristics, P<sub>0</sub>, P<sub>1</sub>, P<sub>3</sub>, P<sub>4</sub>, P<sub>7</sub>, P<sub>9</sub>, and P<sub>10</sub> cells were seeded on poly-L-lysine-coated 8-well chamber slides (BD Biosciences), cultivated for another 1–2 days and subjected to immunocytochemistry and immunofluorescence studies.

#### Immunofluorescence staining

Samples were rinsed briefly in PBS, fixed in ice-cold methanol for 10 min and were then allowed to dry completely. After permeabilization with 0.025% Triton X-100 (Merck, Darmstadt, Germany), cells were incubated with 1.5% normal goat or donkey blocking serum (Santa Cruz Biotechnology) in PBS for 30 min at 37°C to suppress non-specific binding of IgG. After washing the cells three times with PBS (5 min each), cells were incubated overnight at 4°C

with the primary antibodies listed in Table 1. After three PBS washes, cells were incubated with FITC and Texas red (Santa Cruz Biotechnology) labelled appropriate secondary antibodies for 25 min in the dark. After washing three times with PBS in the dark, cells were mounted with mounting medium containing DAPI (Santa Cruz Biotechnology).

#### Immunocytochemistry

Immunocytochemistry analysis was performed using the streptavidin-peroxidase method (UltraVision Plus Large Volume Detection System Anti-Polyvalent, HRP immunostaining Kit, Thermo Scientific, UK). To reduce nonspecific background staining due to endogenous peroxidase, cultured cells were fixed in ice-cold methanol with 0.3% hydrogen peroxide (Carlo Erba Reactifs, Val-De-Reuil Cedex Pa Des Portes, FRANCE) for 15 min and allowed to dry. After additional PBS washes, cells were incubated with Ultra V Block for 5 min at room temperature. Then, cells were incubated overnight at 4°C with the primary antibodies listed in Table 1. The following day, cells were incubated with biotinylated secondary antibodies for 15 min at room temperature. Incubations were followed by streptavidin peroxidase treatment for 15 min. at room temperature and signals were detected with the AEC kit (Zymed Laboratories, UK). The cells were counter-stained with haematoxylin (Santa Cruz Biotechnology) and were examined under a light/fluorescent microscope (Leica DMI 4000B, Wetzlar, Germany).

#### Cell proliferation and viability-MTT Test

The proliferation rate of hNDP-SCs and hBM-MSCs was determined by MTT. MTT was analysed using the MTT Cell Growth Kit (Chemicon) on passage three cultures of MSCs. MSC suspensions were seeded at 12,500 cells/well in 6-well plates (for 1, 4, 7, and 11 days) and T25 flasks (for 14, 17, and 21 days) and were incubated in 5% CO<sub>2</sub> at 37°C for 1, 4, 7, 14, 17, and 21 days. Next, the culture medium was replaced. Wells were washed twice with PBS. In the growth curve experiment, 10  $\mu$ l MTT (0.5 mg/ml) was added to the culture for an incubation time of 4 h. Culture medium was discarded and replaced with 100  $\mu$ l isopropanol/HCl. Absorbance at 570 nm was measured by a UV-visible spectrophotometer microplate reader (VersaMax, Molecular Device, USA). For each group, experiments were repeated three times and measurements were completed in triplicate.

#### Reverse transcription-polymerase chain reaction (RT-PCR)

Total RNA was isolated from  $3 \times 10^6$  MSCs derived from natal teeth and bone marrow at passage 4 by the High Pure

**Table 1** Immunocytochemical properties of hNDP-SCs and hBM-MSCs

Antibody/marker	Dilution	Source	Cell type	
			<i>hNDP-SCs</i>	<i>hBM-MSCs</i>
			Detection	Detection
CD 31/ PECAM-1 (M-20)	1:100	Santa Cruz Biotechnology	∅	∅
CD 34 (C-18)	1:150	Santa Cruz Biotechnology	∅	∅
CD 44/HCAM (Ab-4)	1:150	Thermo Scientific	+	+
CD 45 (H-230)	1:150	Santa Cruz Biotechnology	∅	∅
CD 71 (K-20)	1:150	Santa Cruz Biotechnology	∅	∅
CD105/Endoglin (M-20)	1:100	Santa Cruz Biotechnology	+	+
c-Fos (4)	1:50	Santa Cruz Biotechnology	+	+
Collagen II Ab-2 (2B1.5)	Prediluted	Thermo Scientific	+	+
Collagen Ia1 (D-13)	1:50	Santa Cruz Biotechnology	+	+
$\beta$ - Tubulin (KMX-1)	1:50	Chemicon International	+	+
$\beta$ -Tubulin	Prediluted	Thermo Scientific	+	+
Nestin (Rat-401)	1:50	Santa Cruz Biotechnology	+	+
Vimentin (C-20)	1:100	Santa Cruz Biotechnology	+	+
Desmin Ab1 (D33)	Prediluted	Thermo Scientific	+ <sup>a</sup>	+ <sup>a</sup>
Fibronectin (EP5)	1:100	Santa Cruz Biotechnology	+	+
$\alpha$ -Smooth Muscle Actin Ab-1	1:800	Thermo Scientific	+	+
Actin (C-2)	1:50	Santa Cruz Biotechnology	+	+
MyoD (4H207)	1:50	Santa Cruz Biotechnology	∅	∅
Myosin IIa (A4.74)	1:50	Santa Cruz Biotechnology	+	+
Myogenin Ab-1 (F5D)	Prediluted	Thermo Scientific	+	+
MAP 2a,b Ab-2 (AP20)	Prediluted	Thermo Scientific	+	+
GFAP Ab1	Prediluted	Thermo Scientific	+	+
$\beta$ 3Tubulin (2Q121)	1:50	Santa Cruz Biotechnology	+	+
NSE/ $\gamma$ Enolase	1:500	Chemicon International	+	+
Osteocalcin (FL-100)	1:50	Santa Cruz Biotechnology	+	+
Osteonectin (SPARC)	1:50	Chemicon International	+	+
Osteopontin (AKM2A1)	1:50	Santa Cruz Biotechnology	+	+
BMP-2 (N-14)	1:50	Santa Cruz Biotechnology	+	+
BMP-4 (N-16)	1:50	Santa Cruz Biotechnology	+	+
MEPE (LFMb-33)	1:50	Santa Cruz Biotechnology	∅	∅

+ Positive marker expression; ∅ lack of marker expression; -/+ weak marker expression

<sup>a</sup> Immunoreactivity was positive in 10–20% of the cells

RNA Isolation Kit (Roche, Mannheim, Germany). After the isolation, the RNA concentrations were measured at 260 nm using a Nanodrop spectrophotometer (Thermo SCIENTIFIC). One microgram of total RNA was reverse-transcribed into cDNA using the Transcriptor High Fidelity cDNA Synthesis Kit (Roche, Mannheim, Germany) with both oligo (dT) and random hexamers. The cDNA synthesis reaction was carried out immediately after RNA isolation and the reaction mix consisted of 5  $\mu$ g of RNA, 1 mM of dNTPs, 0.2  $\mu$ g of primers, 20 units of riboblock inhibitor and 200 units of M-MuLV reverse transcriptase. The RNA, primer, and dNTP mixture was denatured for 1 min at 90°C. The temperature was lowered to 42°C before the addition of M-MuLV RT enzyme plus riboblock inhibitor.

The reaction ran for 1 h at 42°C. For the second strand synthesis, PCR was performed with a PCR enzyme mix (Fermentas, USA). The sense and antisense primers used are listed in Table 2. The 25  $\mu$ L PCR reaction mixture consisted of 1  $\times$  PCR buffer, 0.2 mM of each dNTP, 0.5  $\mu$ M of each primer, 1.25 mM MgCl<sub>2</sub>, 1.5 units of Taq DNA polymerase, and 2  $\mu$ L of the first strand cDNA reaction. An initial 5 min denaturation step at 94°C was followed by cycles including denaturation at 94°C, annealing at an appropriate temperature and elongation at 72°C. PCR reactions ended with a final elongation step at 72°C. PCR products were analysed by agarose gel electrophoresis. The name and sequences of the primers, the sizes of PCR products, and annealing temperature for each pair are listed in Table 2.

**Table 2** RT-PCR primers used in this study

Genes	Forward primer (F) Reverse primer (R)	GeneBank accession no.	Size of PCR product (bp)	Annealing temperature (°C)
<b>Rex-1</b> (RNA exonuclease 1)	F: GGATCTCCACCTTTCCAAG R: GCAGGTAGCACACCTCTG	NM_020695	104	54
<b>Oct-4</b> (Pou5f1; POU class 5 homeobox 1)	F: TGCCGTGAAACTGAAGAAG R: TTTCTGCAGAGCTTTGATGTTC	NM_203289	72	53
<b>NANOG</b>	F: CCTCTTAAATTTTTCTCTCTCTTC R: AAGTGGGTTGTTTGCCTTTG	NM_24864	271	52
<b>ACTA2</b> (smooth muscle actin, alpha 2)	F: ATGAGGGCTATGCCTTGCCC R: CCCGATGAAGGATGGCTGGA	NM_001613	307	57
<b>ACTB</b> (actin, beta)	F: TGGCACCACACCTTCTACAATGAGC R: GCACAGCTTCTCTTAATGTCAACG	NM_001101	395	59
<b>Desmin</b>	F: CAGGTGGAGATGGACATGTCTAAGC R: TCATCTCCTGCTTGGCCTGG	NM_001927	186	55
<b>MYOD1</b> (Myogenic differentiation 1)	F: GCCGCTGAGCAAAGTAAATGAGG R: TAGTCCATCATGCCGTCGGAGC	NM_002478	280	53
<b>NEFH</b> (Neurofilament, heavy polypeptide 200 kDa)	F: GAACACAGACGCTATGCGCTCAG R: CACCTTTATGTGAGTGGACACAGAG	NM_021076	396	54
<b>NEFL</b> (Neurofilament, light polypeptide 68 kDa)	F: TCCTACTACACCAGCCATGT R: TCCCAGCACCTTCAACTTT	NM_006158	283	54
<b>TUBB3</b> (tubulin, beta 3)	F: CATGGACAGTGTCCGCTCAG R: CAGGCAGTCGCAGTTTTCAC	NM_006086	175	58
<b>Enolase 2</b> (gamma, neuronal; ENO2)	F: TTATTGGCATGGATGTTGCTGC R: CCCGCTCAATACGTTTTGGG	NM_001975	269	55
<b>Nestin</b>	F: CTCTGACCTGTCAGAAGAAT R: GACGCTGACACTTACAGAAT	NM_006617	302	54
<b>COMP</b> (Cartilage oligomeric matrix protein)	F: CCGACAGCAACGTGGTCTT R: CAGGTTGGCCAGATGATG	NM_000095	91	53
<b>SOX9</b> SRY (sex determining region Y)-box 9	F: TGAAGAAGGAGAGCGAGGAA R: GGGGCTGGTACTTGTAAATCG	NM_000346	348	53
<b>c-fos</b>	F: AGAATCCGAAGGGAAAGGAA R: CTTCTCCTTCAGCAGGTTGG	NM_005252	149	55
<b>OPN</b> (osteopontin) (secreted phosphoprotein 1;SPP1)	F: CAGTGACCAGTTCATCAGATTCATC R: CTAGGCATCACCTGTGCCATAACC	NM_001040058	374	55
<b>OCN</b> (osteocalcin) (bone gamma-carboxyglutamate protein)	F: ATGAGAGCCCTCACACTCCT R: CAAGGGGAAGAGGAAAGAAG	NM_199173	377	54
<b>Runx2</b> (runt-related transcription factor 2)	F: CAGACCAGCAGCACTCCATA R: CAGCGTCAACACCATCATT	NM_004348	177	57
<b>MEPE</b> (matrix extracellular phosphoglycoprotein)	F: GCTGTGTGGAAGAGCAGAGG R: TCATCTCCATCCTCAAACCC	NM_020203	303	53
<b>Osteonectin</b>	F: TCTTCCCCTGTACACTGGCAGTTC R: AGCTCGGTGTGGGAGAGGTA	NM_003118	73	55
<b>Vimentin</b>	F: AAGCAGGAGTCCACTGAGTACC R: GAAGGTGACGAGCCATTTC	NM_003380	205	55
<b>ADFP</b> (Adipophilin)	F: CGCTGTCACTGGGGCAAAGA R: ATCCGACTCCCAAGACTGTGTTA	NM_001122	173	59
<b>Leptin</b>	F: GTAGAGTTTGAAGGAGGTGA R: CTGGGAATTAGCCATTGTG	NM_000230	348	54
<b>Adiponectin</b>	F: ATGGTCCTGTGATGCTTTGA R: GTTGAGTGCATGTTATTTT	NM_004797	229	54
<b>PPAR<math>\gamma</math></b> (peroxisome proliferator-activated receptor gamma)	F: CAGTGGGGATGCTCATAA R: CTTTTGGCATACTCTGTGAT	NM_138711	422	54

### Real-time polymerase chain reaction

RNA isolation and cDNA synthesis was performed as described above. Equal amounts of cDNA were used for the real-time amplification of the target genes using UPL Prob (Universal Prob Library) according to the manufacturer's recommendations on the LightCycler 480-II (Roche Diagnostic) real-time quantitative PCR instrument.

The relative gene expression of the housekeeping gene, HPRT (Hypoxanthine-guanine phosphoribosyl transferase), and relative target gene expression of Nanog, Oct4, Sox2, FoxD3 and Rex-1 were determined. Primers used for real-time PCR were as follows: Nanog (Nanog homeobox) forward 5'-ATG CCT CAC ACG GAG ACT GT-3' and reverse 5'-AGG GCT GTC CTG AAT AAG CA-3'; Rex1 (RNA exonuclease 1) forward 5'-GGA TCT CCC ACC TTT CCA AG-3' and reverse 5'-GCA GGT AGC ACA CCT CCT G-3'; Oct4 forward 5'-TGC CGT GAA ACT GGA GGA G-3' and reverse 5'-TTT CTG CAG AGC TTT GAT GTT C-3'; Sox2 (HGNC transcription factor) forward 5'-ATG GGT TCG GTG GTC AAG T-3' and reverse 5'-GGA GGA AGA GGT AAC CAC AGG-3'; and FoxD3 (fork-head box D3) forward 5'-CCA ATT TCC TTT CCC CTG AG-3' and reverse 5'-TCG ACC AGC TTA GGT GTG C-3'. Primers and probes from the pre-developed kits were added according to manufacturer's instructions (0.4 µl reference probe, 0.4 µl target probe, 0.4 µl reference primer mix, 0.4 µl target forward primer mix (L), 0.4 µl target reverse primer mix (R), 10 µl master mix and 3 µl water). PCR conditions were as follows: incubation for 10 min at 95°C, followed by 45 cycles of 10 s denaturation at 95°C, annealing for 30 s at 60°C and 1 s extension at 72°C. The target and reference genes were amplified in the same wells. The reaction mixture, lacking cDNA, was used as a negative control in each run. In addition, cDNA reaction mix without template was used as a negative control. Expression of HPRT was used as reference.

### Real-time PCR data analysis

Results were analysed with Light Cycler software (version 4). The crossing points were assessed and were plotted versus the serial dilution of known concentrations of standards derived from each gene by the Fit Points method. PCR efficiency was calculated by the Light Cycler Software, and the data were only used if the calculated PCR efficiency ranged from 1.85–2.0.

### Telomerase activity

Telomerase activity was determined with the conventional telomeric repeat amplification protocol (TRAP) using the TRAP TeloTAGGG PCR enzyme-linked immunosorbent

assay (ELISA) kit (Roche, Mannheim, Germany) according to the manufacturer's protocol. Briefly,  $2 \times 10^5$  cells were washed with phosphate-buffered saline (PBS) and homogenised in 200 µl of ice-cold lysis buffer. The homogenate was incubated on ice for 30 min and centrifuged at  $16,000 \times g$  for 20 min at 4°C. The supernatant was collected and cell extracts were incubated with mixed buffer containing a biotin-labelled primer, one unlabelled primer, dNTPs and Taq DNA polymerase. This reaction ran for 20 min at 25°C and allowed telomerase to add the telomeric repeats to the end of the biotin-labelled synthetic primer. The products were extended by incubation at 94°C for 5 min, followed by 30 cycles of 94°C, 30 s; 50°C, 30 s; 72°C, 90 s; and a final extension at 72°C for 10 min. To detect the telomeric repeat-specific sequence, the products were denatured and mixed with a digoxigenin (DIG)-labelled probe. The mixture was incubated in the streptavidin-coated wells of the microplate. Finally, the DIG-labelled hybrids were visualised with a peroxidase conjugated anti-DIG antibody and a substrate (TMB) and quantified photometrically at 450 nm with a reference wavelength of 690 nm. Relative telomerase activity is calculated as the ratio of the absorbance value of the sample to that of the control.

### In vitro differentiation

#### *In vitro adipogenic differentiation*

Cells from passage three (3,000 cells/cm<sup>2</sup>) were seeded onto coated type I collagen coverslips (BD Biosciences) in 6-well plates to induce adipogenic differentiation. The adipogenic medium, MEM (Invitrogen/GIBCO), was supplemented with 10% FBS (Invitrogen/GIBCO), 0.5 mM isobutyl-methylxanthine (IBMX-Sigma-Aldrich),  $10^{-6}$  M dexamethasone (Sigma-Aldrich, Fluka Chemie AG, Buchs, Switzerland), 10 µg/ml insulin (Invitrogen/GIBCO), 200 µM indomethacin (Sigma-Aldrich), and 1% antibiotic/antimycotic (Invitrogen/GIBCO) for 4 weeks. The medium was replaced twice a week. The presence of intracellular lipid droplets, which indicates adipogenic differentiation occurred was confirmed by Oil Red O (Sigma-Aldrich) staining with 0.5 % oil red O in methanol.

#### *In vitro osteogenic differentiation*

Cells from passage three (3,000 cells/cm<sup>2</sup>) were seeded onto 6-well plates with type I collagen coated coverslips. For osteogenic differentiation, MEM (Invitrogen/GIBCO) was supplemented with 100 nM dexamethasone (Sigma-Aldrich), 0.05 µM ascorbate-2-phosphate (Wako Chemicals, Richmond, VA, USA), 10 mM β-glycerophosphate (Sigma-Aldrich), 1% antibiotic/antimycotic and 10% FBS (Invitrogen/GIBCO) and the cells were incubated in this

medium for four weeks. The medium was replaced twice a week. At the end of the fourth week, osteogenic differentiation was assessed via staining with Alizarin Red (Sigma-Aldrich, Fluka Chemie AG, Buchs, Switzerland) and immunocytochemical staining of osteocalcin, osteopontin, osteonectin, BMP-2 and BMP-4.

#### *Alizarin red staining*

Cells were plated and induced for osteogenic differentiation as described. Briefly, excess medium was decanted and cells were fixed for 5 min at room temperature in ice-cold 70% ethanol and were then allowed to dry completely. Cells were stained with alizarin red solution composed of 2% alizarin red S (pH value of the alizarin red S solution was adjusted to 4.1–4.3 with ammonium hydroxide) for 30 s to 1 min., then washed with distilled water (20 dips). Excess dye was poured out and stained cells were dehydrated in acetone (20 dips), fixed in acetone-xylene (1:1) solution (20 dips), cleared with xylene (20 dips), dried completely, and mounted in mounting medium.

#### *Alkaline phosphatase activity*

Cell alkaline phosphatase (ALP) activity was determined at days 3, 7, 11, 14, 21, and 28 as a method to assess osteogenic differentiation. Cell layers were washed three times with PBS and total protein was extracted by Mammalian Protein Extract Reagent (M-PER) (Thermo Scientific). The *p*-Nitrophenyl Phosphate Liquid Substrate (Sigma Aldrich, N7653) was used to detect ALP activity. The cells were incubated at room temperature with *p*-Nitrophenyl Phosphate for 30 min. The optical density of the yellow product, para-nitrophenol, was determined by a VersaMax Microplate Reader (Molecular Devices) at 405 nm. Protein concentration of the cell lysate was measured via the Bicinchoninic Acid Protein Determination method (Sigma-Aldrich) (Wu et al. 2007) and ALP activity was expressed as OD 405 nm/mg of protein (Wu et al. 2007). Three technical replicates of each sample were analysed.

#### *In vitro chondrogenic differentiation*

To induce chondrogenic differentiation,  $2.5 \times 10^5$  cells were transferred into a 15-mL polypropylene tube and were centrifuged at  $1300 \times g$  for 5 min to form a pelleted micromass. The micromass was cultured with chondrogenic medium for 2 weeks. The medium was changed twice a week. Chondrogenic medium consists of high-glucose DMEM (Gibco-BRL, Grand Island, NY, USA) supplemented with 10 ng/ml transforming growth factor- $\beta$ 1 (TGF- $\beta$ 1; Biosource PHG0021), 50  $\mu$ g/ml

ascorbate-2-phosphate (Wako Chemicals, Richmond, VA, USA), 0.1  $\mu$ M dexamethasone (Sigma-Aldrich, Fluka Chemie AG, Buchs, Switzerland), 100  $\mu$ g/ml sodium pyruvate (Sigma-Aldrich, St. Louis, MO, USA), 40  $\mu$ g/ml proline (Merck, Darmstadt, Germany), 50 mg/ml ITS premix (BD Biosciences, Bedford, MA), and 1% antibiotic/antimycotic (Gibco-BRL, Grand Island, NY, USA). The pellets, fixed with 4% paraformaldehyde and embedded in paraffin, were stained with Haematoxylin–Eosin, Alcian blue and Safranin O to assess chondrogenic differentiation.

#### *In vitro myogenic differentiation*

To induce myogenic differentiation, MSCs from passage three were seeded on collagen-coated coverslips. After 24 h of incubation, the medium was replaced with high glucose Dulbecco's modified Eagle's medium (H-DMEM) supplemented with 5% horse serum and 10 mM 5-azacytidine. The cells were allowed to grow in this medium for 24 h and were washed twice with PBS. To allow further growth, the cells were cultured in H-DMEM containing 5% horse serum, 50 mM hydrocortisone and 4 ng/ml basic fibroblast growth factor. In order to assess myogenic differentiation, cells were stained with antibodies against MyoD, Myosin IIa, desmin, myogenin and  $\alpha$ -SMA.

#### *In vitro neurogenic differentiation*

MSCs from passage three were seeded on collagen-coated coverslips to induce neurogenic differentiation. After the cells were 70% confluent, they were cultured for 3–5 days with low glucose Dulbecco's modified Eagle's medium (L-DMEM) containing 0.5 mM isobutylmethylxanthine (IBMX), 10 ng/ml brain-derived neurotrophic factor (BDNF), epidermal growth factor (EGF), basic fibroblast growth factor ( $\beta$ -FGF), neural stem cell proliferation supplements (Stem Cell Technologies Inc.) and 1% penicillin–streptomycin (Gibco-BRL). Differentiation was assessed by immunohistochemical staining of GFAP, HNK-1ST, neurofilament (Thermo Scientific), tubulin- $\beta$ , tubulin  $\beta$ -III, c-Fos, nestin, and  $\gamma$ -enolase (Santa Cruz Biotechnology).

#### *Statistical analysis*

All experiments were repeated a minimum of three times. Data are reported as mean  $\pm$  SD and all statistical analyses were performed using SPSS 10.0. In addition, data were analysed using one-way ANOVA and the paired *t* test. Differences between the experimental and control groups were regarded as statistically significant when  $p < 0.05$ .

## Results

### Cultures of hNDP-SCs and hBM-MSCs

A sparse number of hNDP-SCs attached to culture flasks and the majority of cells displayed a fibroblast-like, spindle-shaped morphology during the early days of incubation. These cells began to proliferate after 3–4 days of incubation and gradually grew to form small colonies, named colony forming units (Fig. 1a). After plating for 12–15 days, these primary cells reached 80% confluence during their first passage. During their later passages, the majority of these SCs exhibited large, flattened or fibroblast-like morphology (Fig. 1b, c). No changes in morphology and growth were observed throughout the 25 passages. Moreover, cells that were stored long-term at  $-80^{\circ}\text{C}$  demonstrated high vitality and capability to quickly restart proliferation and tissue production and were capable of retaining their differentiation potential after long-term storage. Similarly, hBM-MSCs displayed a fibroblast-like, spindle-shaped morphology during their early days of incubation (Fig. 1d). These primary cells reached 70–80% confluency after 12–15 days of incubation during their early passages. During later passages, the cell morphology changed and the majority of cells exhibited large, flattened or fibroblast-like morphology (Fig. 1e, f).

### Ultrastructural characteristics

Electron microscopy showed pale, eccentric, irregularly shaped and large euchromatic nuclei with one or more

nucleoli located near the perinuclear cisternae (Fig. 2a, b). Two distinct areas were clearly observed in the cytoplasm: (a) an intensely stained inner zone that was rich with mitochondria and rough endoplasmic reticulum (rER) cisternae and (b) a thin to thick changeable relatively peripheral zone which was poor for organelles (Fig. 2a–d). Interestingly, the rER cisternae were distended and contained moderately electron-dense material (Fig. 2c). Aggregates containing lipid droplets, granules and glycogen were also observed. Numerous thin pseudopodia were observed on the cell surface (Fig. 2a–d).

### Flow cytometry-identification of hNDP-SCs and hBM-MSCs

Defined markers exist that specifically and uniquely identify MSCs. We utilised some markers to define our cultured cells. Our data indicated that hNDP-SCs and hBM-MSCs expressed CD13, CD44, CD73, CD90, CD146, and CD166, but not CD3, CD8, CD10, CD11b, CD14, CD15, CD19, CD33, CD34, CD45, CD71, CD117, and HLA-DR. These findings are consistent with their undifferentiated state, and as similar to hBM-MSCs, they possessed immunophenotypic MSC characteristics (Fig. 3a, b).

### Growth characteristics of hNDP-SCs

Under the culture conditions used in this study, hNDP-SCs were consistently grown for more than 25 passages without losing their proliferative ability. The data from the MTT assay showed that the mean percentage of formazan

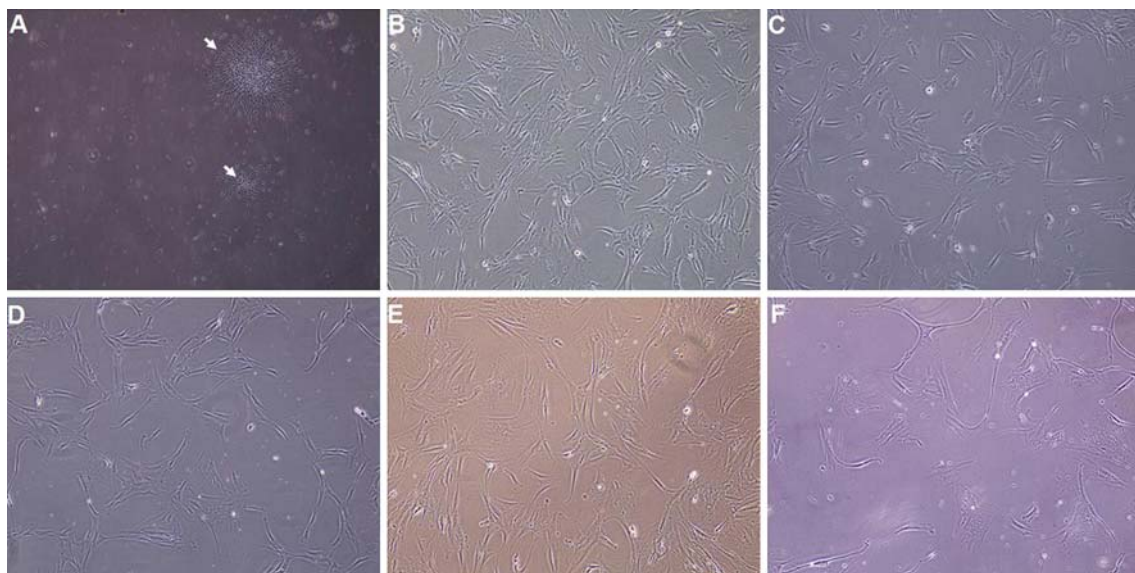


**Fig. 1** Morphology of hNDP-SCs and hBM-MSCs. During the onset of culture (P0—2nd day, **a**), the isolated cells from natal teeth dental pulp formed single-cell-derived colonies (*arrows*). After the next passages, most of these SCs exhibited large, flattened or fibroblast-like

morphology (**c** P1—5th day; **d** P22—4th day) similar to hBM-MSCs (**d** P0—2nd day; **e** P1—12th day, **f** P22—2nd day) (Original magnification: **a** X48; **b–f**  $\times 100$ )



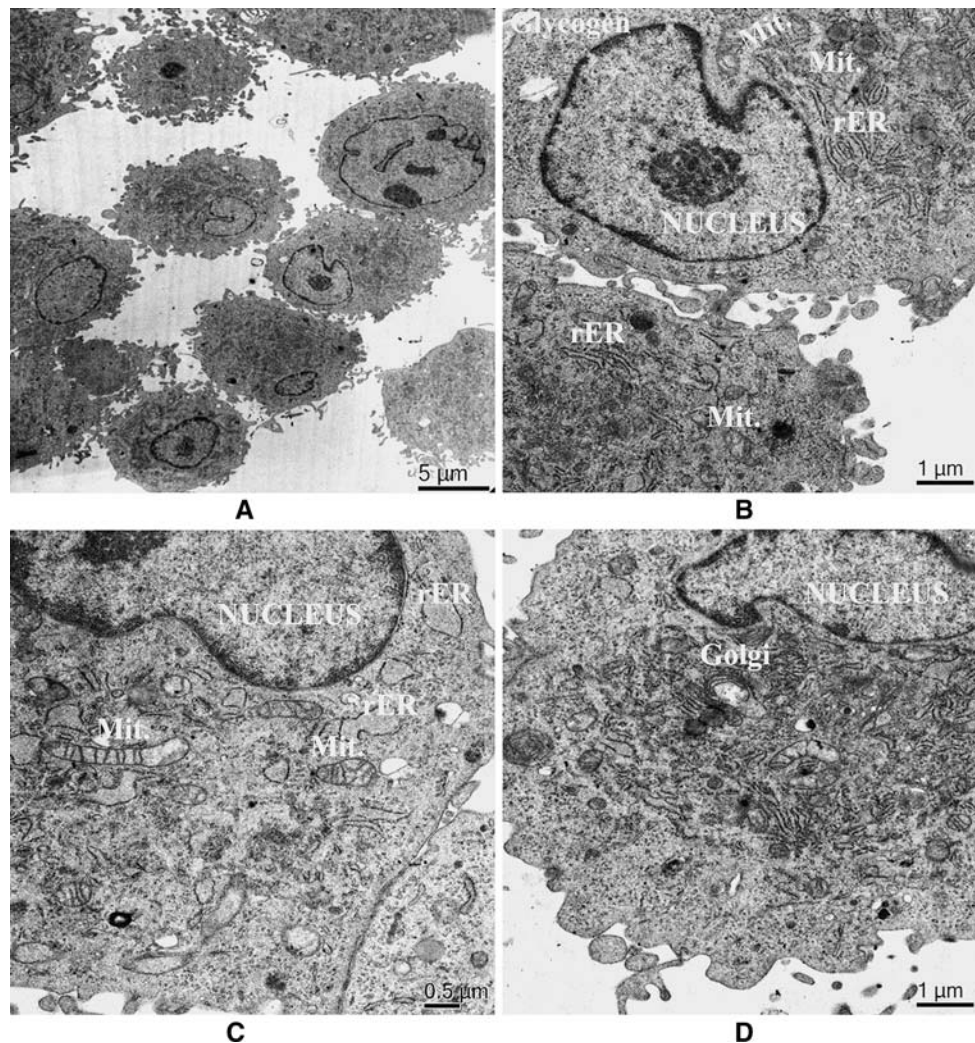


**Fig. 2** Electron microscopic analysis of hNDP-SCs. The cells show pale, eccentric, irregularly shaped large nuclei, usually with multiple nucleoli (**a, b**). Plasma membrane has many thin pseudopodia (**a, b, d**). The cytoplasm has many rough endoplasmic reticulum (rER) cisternae

with dilated and contained electron-dense material, mitochondria (Mit), Golgi apparatus (Golgi) (**b, c, d**). We can see well-developed glycogen aggregates were also observed in cytoplasm (**b**)

absorbance values (OD values) increased as demonstrated in Fig. 4. In addition, hNDP-SCs had a better proliferation capacity than hBM-MSCs (Fig. 4).

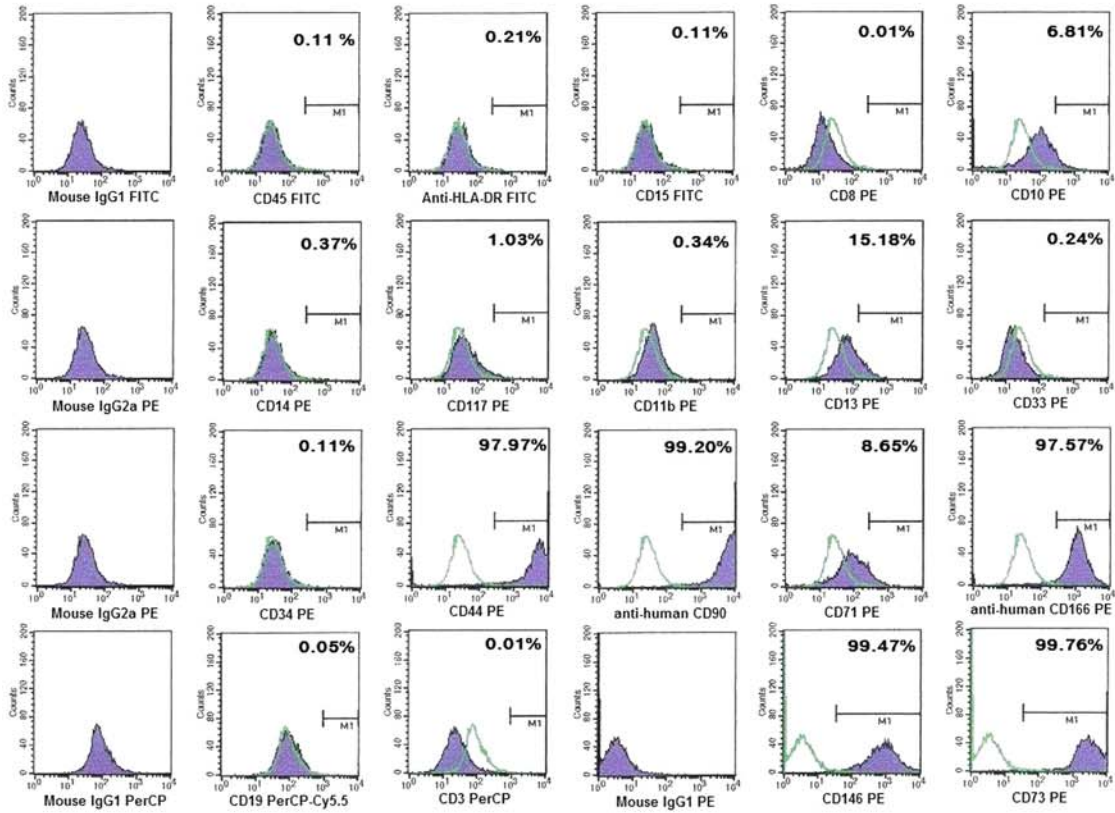
#### Immunocytochemistry-identification of hNDP-SCs

Figures 5 and 6 depict immunocytochemical staining of hNDP-SCs. Typical immunoreactivity profiles of hNDP-SCs and hBM-MSCs are specified in Table 1. Vimentin is a popular cytoplasmic marker used to denote MSCs and it was expressed throughout the cell passages in this study (Fig. 6a). Under the standard culture conditions, these cells expressed other MSC markers such as CD44 (Fig. 5f), CD105/endoglin (Fig. 5h) and fibronectin (Fig. 6c) and their morphological characteristics remained unchanged. As summarised in Table 1, hNDP-SCs and hBM-MSCs did not express other surface markers such as CD31 (endothe-

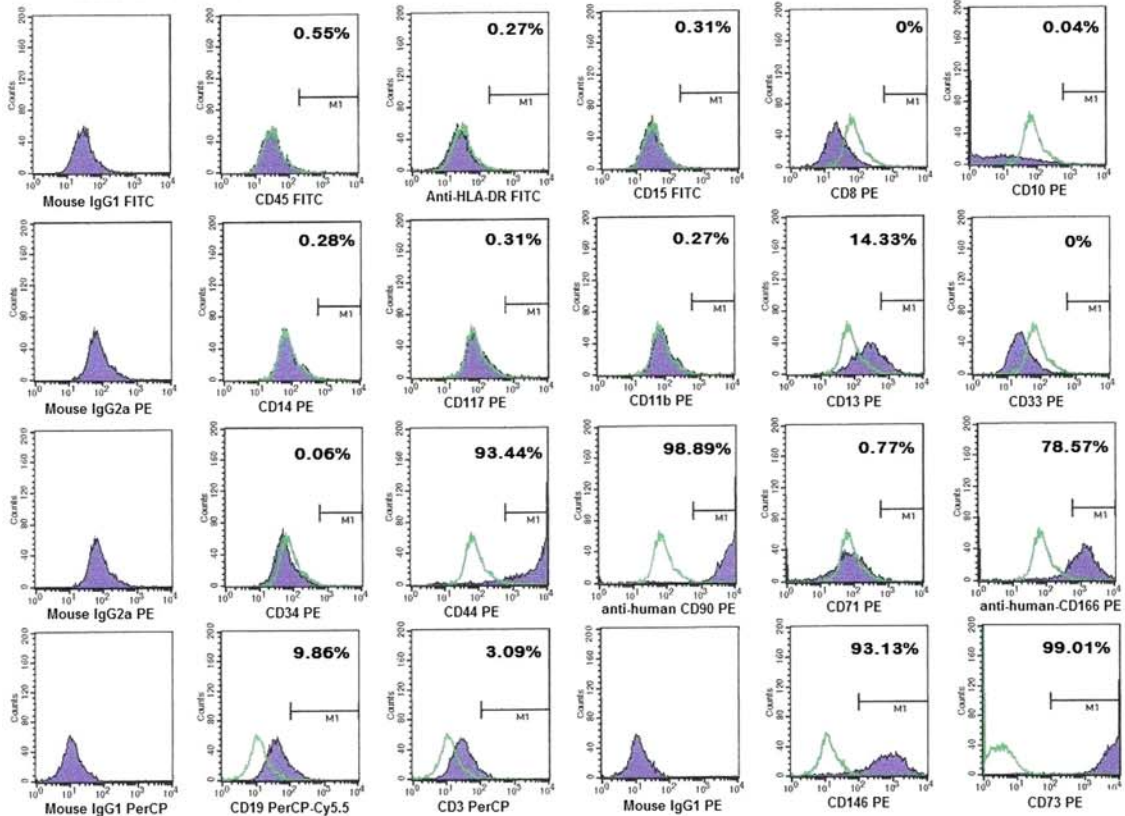
lial), CD34 (Fig. 5e), CD45 (Fig. 5g) (hematopoietic markers) and CD71 (transferrin receptor).

Osteoblastic cells can be characterised both in vitro and in vivo by the specific expression of osteocalcin and osteonectin and by the strong secretion of type I collagen and osteopontin. However, we surprisingly observed strong expression of type I (Fig. 5j) and II collagen (Fig. 5i), osteocalcin (Fig. 5k), osteonectin (Fig. 5l), BMP-2 and BMP-4 (data not shown) in the hNDP-SCs and hBM-MSCs cultured in regular growth medium. To our knowledge, this study is the first report demonstrating a positive immune reaction with osteocalcin, osteonectin osteopontin, BMP-2 and BMP-4 in hNDP-SCs and hBM-MSCs. In addition, hNDP-SCs that were not stimulated towards differentiation, expressed some myogenic markers such as desmin (Fig. 5c), myogenin (Fig. 5d),  $\alpha$ -SMA (5A) and myosin IIa (data not

**A hNDP-SCs-P3**



**B hBM-MSCs-P3**



◀ **Fig. 3** Representative flow cytometry analysis of cell-surface markers in hNDP-SCs (a) and hBM-MSCs (b) at the passage 3. Cells were labelled with antibodies against hematopoietic antigens (CD3, CD8, CD10, CD14, CD15, CD33, CD34, CD45, CD71, CD117 and HLA-DR) and MSC markers (CD13, CD44, CD73, CD90, CD146 and CD166) or immunoglobulin isotype antibodies and analysed by flow cytometry as above. *Green line*, control immunoglobulin

shown), and chondrogenic markers including type II collagen (Fig. 5i).

The hNDP-SCs and hBM-MSCs used in this study were positive for GFAP (Fig. 6e), an intermediate filament protein specific for astroglial cells. In addition, they expressed neural progenitor markers such as nestin (Fig. 6d), vimentin (Fig. 6a) and neuronal markers such as c-fos (Fig. 6f), beta III tubulin (Fig. 5f) and  $\gamma$ -enolase, MAP2a,b (data not shown).

#### Gene expression profiles of hND-SCs and hBM-MSCs

##### Reverse transcriptase polymerase chain reaction (RT-PCR)

To determine the self-renewal capacity of hNDP-SCs and hBM-MSCs, the transcript levels of embryonic stem cell genes (Rex-1, Oct4, and Nanog) were determined. In addition to stem cell markers, the expression of differentiation markers, such as osteonectin, osteocalcin, osteopontin and Runx2, which are expressed in precursor osteoblasts, was determined. In addition, adipophilin, leptin, and PPAR $\gamma$  transcript levels, which are expressed in adipoblasts, were determined. Furthermore, the expression of  $\alpha$ -smooth muscle actin ( $\alpha$ -SMA) and desmin, which are expressed in precursor myoblasts, was determined. The expression levels of neurofilament-H and L (NF-H and -L),  $\gamma$ -enolase, nestin and  $\beta$ 3-tubulin, which are expressed in precursor neuroprogenitor

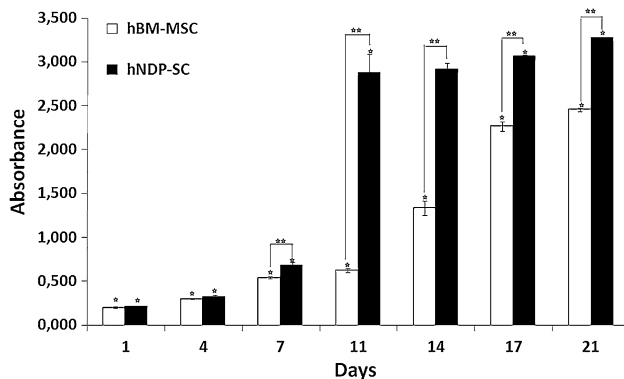


**Fig. 4** Viability/proliferation of hNDP-SCs and hBM-MSCs cultured in MEM medium determined by MTT test. There was 700% increase in live cell number of hNDP-SCs when the data from day 21 was compared with the data from day 1 ( $n = 3$ , mean  $\pm$  SE,  $p < 0.05$ ). There was significantly different at the level of proliferation between hNDP-SCs, and hBM-MSCs during culture ( $n = 3$ , mean  $\pm$  SE,  $p < 0.05$ )

cells, were also determined. The expression of the stem cell and differentiation markers was confirmed in both hNDP-SCs and hBM-MSCs by RT-PCR analysis using specific primer sets (Fig. 7). Our results suggest that hNDP-SCs have stem cell properties.

The presence of cartilage oligomeric matrix protein (COMP) and SOX9, which are expressed in precursor chondroblasts, was also investigated in both cell lines. COMP was slightly expressed in hNDP-SCs but no expression was observed in hBM-MSCs. SOX9 expression was not observed in both cell lines.

##### Real-time PCR

Real-time PCR is a very sensitive detection method; therefore, we utilised it to confirm the RT-PCR results and to demonstrate that the weak bands observed in the RT-PCR were real and present in a quantitative amount. In addition to the transcripts examined by RT-PCR (Rex-1, Oct4, and Nanog), Sox2 and FoxD3 transcripts were also analysed with real-time PCR.

Our real-time PCR data confirmed the reverse transcriptase PCR results and quantified the Oct4, Nanog, Rex-1, FoxD3 and Sox2 transcripts relative to the HRPT house-keeping gene in hNDP-SCs and hBM-MSCs (Fig. 8). Nanog, Oct4, Sox2 and FoxD3 were more highly expressed in hBM-MSCs than in hNDP-SCs while Rex-1 expression was much higher in hNDP-SCs.

##### Telomerase activity of hND-SCs and hBM-MSCs

The telomerase activity of hNDP-SCs was measured at passages 2 (P2) and 15 (P15) and at P3 for the human BM-MSCs. The activities were calculated and normalised with respect to 1  $\mu$ g of total protein. The telomerase activity of hNDP-SCs was  $2.49 \pm 0.13$  amol/ $\mu$ g total protein (P2) ( $n = 3$ ) and  $0.57 \pm 0.12$  amol/ $\mu$ g total protein (P15) ( $n = 4$ ) (Fig. 9) with respect to P2 and P15. The telomerase activity of hBM-MSCs ( $n = 6$ ) could not be detected.

##### Differentiation potential of hNDP-SCs and hBM-MSCs

Histochemical and IHC methods were used to determine the potential of hNDP-SCs to differentiate to adipogenic, osteogenic, chondrogenic, myogenic and neurogenic states.

**Adipogenic differentiation** hNDP-SCs at passages 3–5 were used in the adipogenic differentiation experiments, in which 80–90% sub-confluence was found to be optimal for cell differentiation which lasted for 4–6 weeks. At the start of the fifth week, the lipid droplets enlarged and invaded the entire cytoplasm like adipocyte-differentiated hNDP-SCs (Fig. 10A-a,b,c).

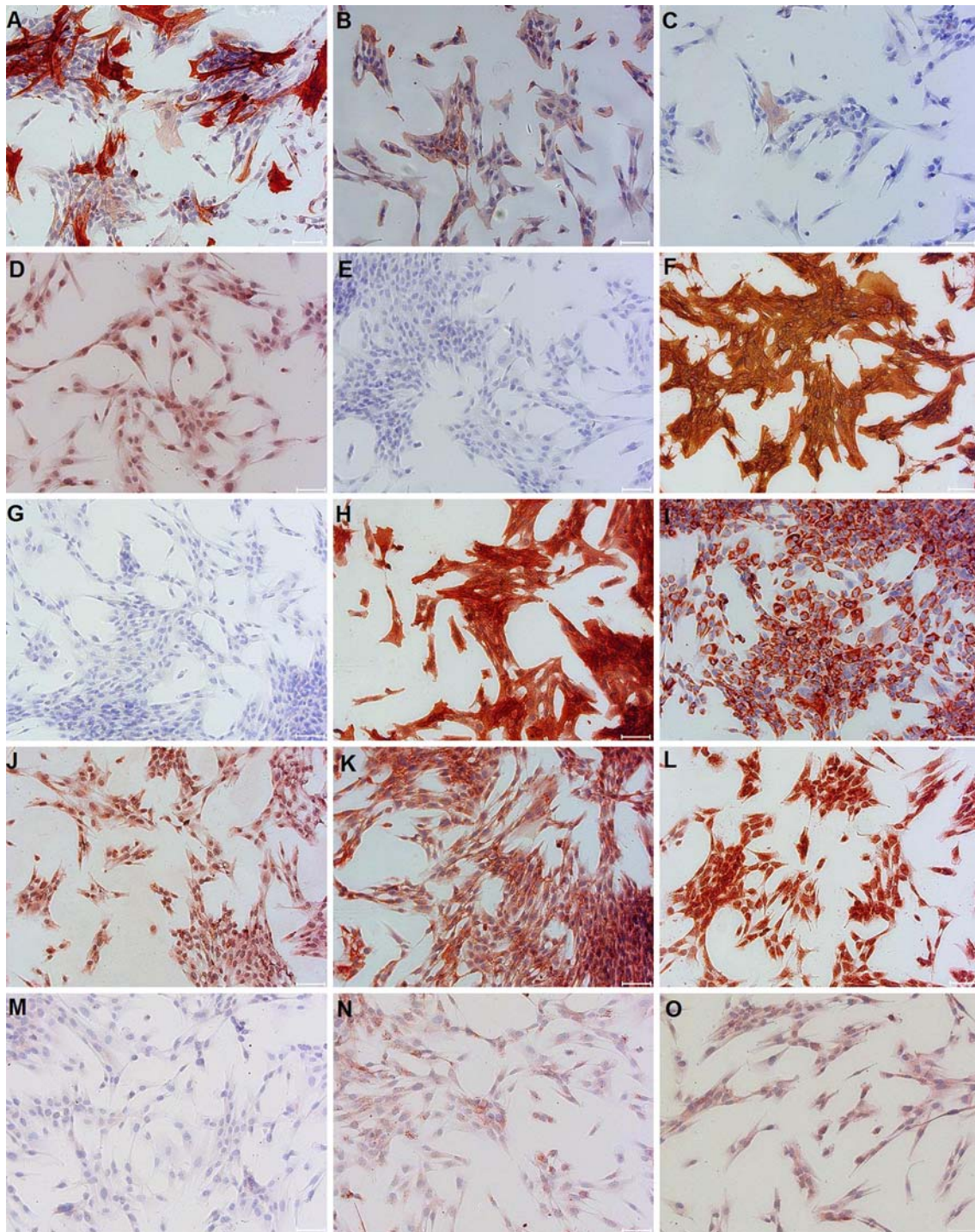


**Fig. 5** Immunophenotype of cultured hNDP-SCs. Studies based on immunoperoxidase reactivity were performed on third passage cultures of hNDP-SCs. Representative staining patterns are shown for:  $\alpha$ -SMA (a), actin (b), desmin (c), myogenin (d), CD 44 (f), CD105 (h), type II collagen (i), type I collagen (j), osteocalcin (k), osteonectin (l),  $\beta$ -tubulin (n) and MAP 2a,b (o). hNDP-SCs did not stain with antibody against CD34 (e), CD45 (g), and MEPE (m). Staining patterns

were as follow:  $\alpha$ -SMA, actin, desmin, type II collagen, osteocalcin, and  $\beta$ -tubulin cytoplasmic, CD44, CD105, type I collagen and MAP2a,b cytoplasmic and membranous, myogenin nuclear, osteonectin cytoplasmic and nuclear. A few number of cells (less than 20 %) stained positive for desmin (e). Nuclei were counterstained with haematoxylin. Control stains negative for each protein were not shown. Scale bars 50  $\mu$ m

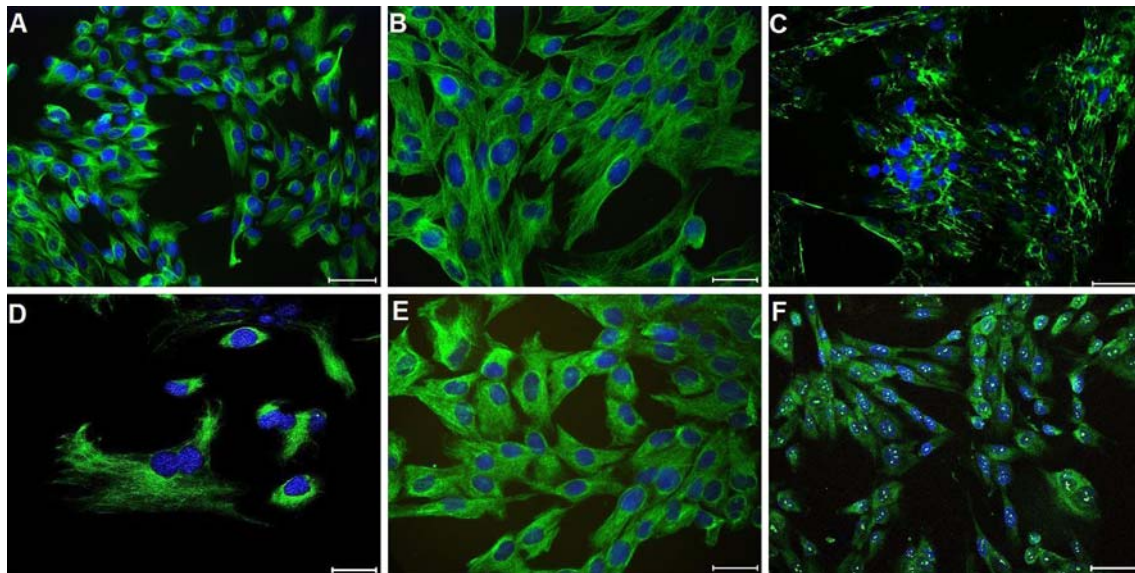


**Fig. 6** Immunofluorescent staining for vimentin (a),  $\beta$ -tubulin (b), fibronectin (c), nestin (d), and GFAP (e) showing exclusive cytoplasmic staining in the hNDP-SCs. c-Fos (f) expression was in cytoplasm and nucleus. Nuclei were labelled with DAPI (blue). Scale bars 30  $\mu$ m



**Fig. 7** Expression of transcripts for embryonic stem cell genes and differentiation markers. mRNA isolated from hNDP-SCs and hBM-MSCs was used for RT-PCR analysis. The expression of stem cell (Rex-1, OCT4, Nanog) and differentiation (alpha-SMA, desmin, NF-H, NF-L, tubulin beta III, enolase, nestin, OPN, OCN, Runx-2, osteonectin,

adipophilin, leptin and PPAR $\gamma$ ) markers were detected. MyoD1, COMP, MEPE and adiponectin were not detected in both cell lines. SOX9 was slightly positive in hNDP-SCs. Internal control:  $\beta$ -actin. Negative control: water

**Osteogenic differentiation** Histo- and/or immunohistochemical techniques that detected bone-specific markers were applied to cells grown in osteogenic differentiation medium and in control medium to assess the osteogenic differentiation of hNDP-SCs. Proliferation and differentiation of both cultures were compared using phase contrast microscopy. In both control and osteogenic cultures, cells proliferated and reached almost complete confluency after 8–10 days of incubation. Later, the cellular aggregates were observed in osteogenic differentiation culture plates and were gradually increased until the completion of the experi-

ment. These aggregates were characterised by the presence of amorphous material deposits (Fig. 10B-a). Alizarin red S stained these nodular aggregates in osteogenic cultures, demonstrating that the amorphous deposits observed at the microscope were actually calcium deposits. Alizarin red positive nodular aggregates were already present at day 28 (Fig. 10B-b, c). At day 38, positive alizarin red aggregates were larger and stained intensively, indicating that a more extensive calcium deposition had occurred. Control cultures showed only minimal background staining (data not shown). Cells that were incubated for 38 days also strongly

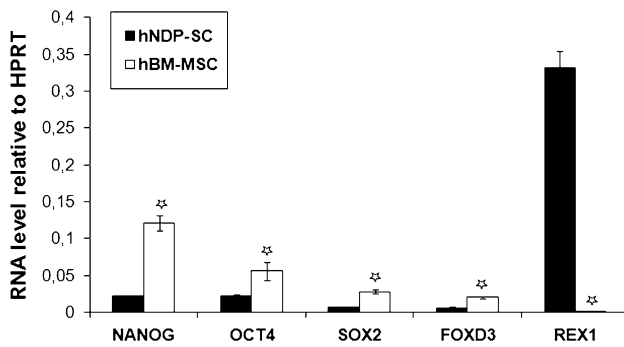


**Fig. 8** Relative expression profiles of Nanog, Oct4, Sox2, FoxD3 and Rex-1 in hNDP-SCs and hBM-MSCs in relation to the expression of a housekeeping gene, HPRT. The data were from triplicate experiments. Asterisk represents  $p < 0.05$

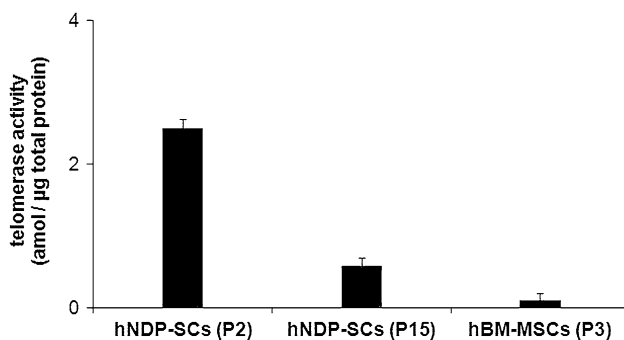


**Fig. 9** Telomerase activities of hNDP-SCs and hBM-MSCs. The telomerase activities of human natal dental pulp SCs passage 2 (P2), passage 15 (P15) and human bone marrow MSCs, passage 3, were estimated by “TRAP TeloTAGGG PCR ELISA” kit (Roche, Mannheim, Germany)

stained positive for osteonectin (Fig. 10B-d), osteopontin (data not shown), osteocalcin (Fig. 10B-d), extracellular located matrix proteins BMP2 (data not shown) and BMP4 (Fig. 10B-f).

**Alkaline phosphatase activity** As a marker for osteoblast differentiation, ALP levels were measured. ALP activity increased in both cell lines following a 7-day incubation in osteogenic differentiation medium when compared with cells exposed to regular growth medium (Fig. 11). ALP activity increased until day 14 and then decreased. The ALP levels of hBM-MSCs were higher than hNDP-SCs. A fourfold increase was observed in ALP activity of undifferentiated hNDP cells during the first 14 days of culturing.

**Chondrogenic differentiation** After 3 weeks, the cell pellets that were induced to differentiate into chondrocytes stained positively with alcian blue (Fig. 10C-c). Histologically, cells observed in the pellets showed several features characteristic of chondrogenic differentiation. Hypertrophic cells were readily identifiable. Furthermore, cells were

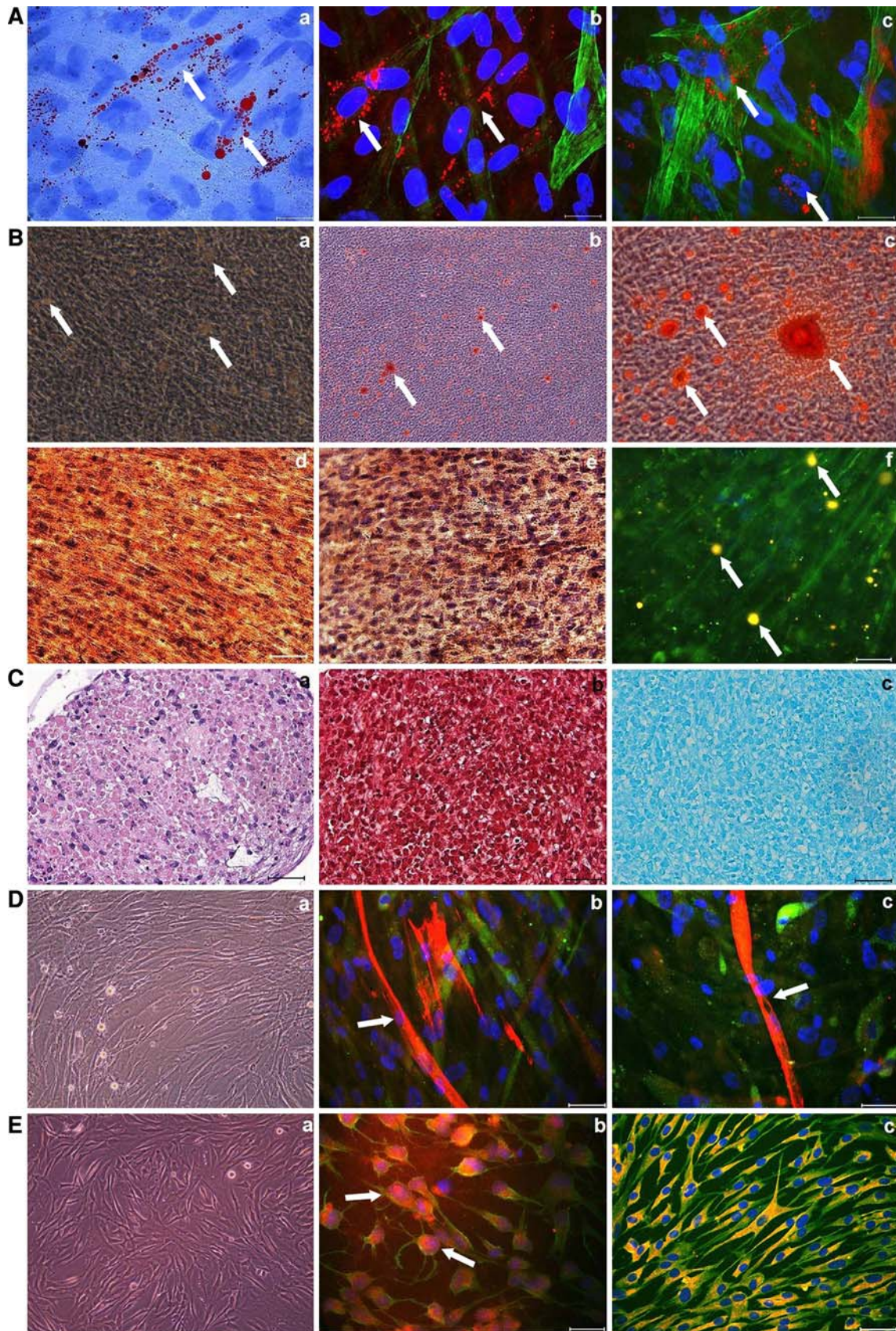
**Fig. 10** Ability of hNDP-SCs to differentiate to multiple lineages. (A) Adipogenic differentiation is visually marked by accumulation of neutral lipid vacuoles in cultures (arrows) (a–c) (red oil staining).  $\alpha$ -SMA expression were shown in green and nuclei in blue with DAPI (b, c) (Scale bars 30  $\mu$ m). (B) Phase-contrast microscopic appearance of the hNDP-SCs differentiated into osteogenic lineage (arrows) at day 38 day (a) (original magnification:  $\times 100$ ). Osteogenic differentiation was indicated by the formation of calcified nodule with alizarin red S staining (arrows) (b, c) (original magnification: b  $\times 40$ ; c  $\times 400$ ). Increased osteonectin (d) and osteocalcin (e) expression were identified in both osteoblast-like cells, which is derived hNDP-SCs and surrounding matrix in osteogenic tissue (Scale bars 50  $\mu$ m). BMP4 is positive in ECM (green) and mineralised bone matrix (arrows) (orange) (f) (Scale bar 50  $\mu$ m). (C) After chondrogenic differentiation, the analysed sections were positive for H–E (a), safranin O (b) and alcian blue (c) staining. Histologically, cells observed in the pellets were round and resembled hyaline chondrocytes, forming cartilaginous lacunae. The presence of GAG is shown by red stain (safranin O) (b). Exposure of hNDP-SCs to TGF $\beta$ 1 during 3 weeks increased in alcian blue staining of ECM (c) (Scale bars 50  $\mu$ m). (D) Myogenic differentiation in vitro: fused hNDP-SCs forming myotubes (arrows) (a) (original magnification:  $\times 100$ ). Positive immunostaining with myoD (nuclear, green) (b), myosinIIa (cytoplasmic, green) (c) and desmin (cytoplasmic, red) (b, c) (Scale bars 50  $\mu$ m). (E) Differentiation of hNDP-SCs to neuro-glial-like cells: phase-contrast microscopic appearance of the hNDP-SCs differentiated into neurogenic lineage at day 2 day (a) (original magnification:  $\times 100$ ). In vitro differentiation of hNDP-SCs into astrocytes (arrows) was shown by GFAP (b) and into neuron-like cells  $\beta$ -tubulin and  $\beta$ -tubulin III (c). c-Fos was normally detected in undifferentiated cells, but its expression was much stronger in differentiated cells (red staining for nuclei) (b) (Scale bars 50  $\mu$ m)

round and resembled hyalin chondrocytes, forming cartilaginous lacunae and were separated by regions of diffuse extracellular matrix (ECM) (Fig. 10C-a–c). Glycosaminoglycans (GAGs) were present and stained red as by Safranin O (Fig. 10C-b). This characteristic histology was not observed in the control cells that were not induced to become chondrocytes (data not shown).

**Myogenic differentiation** hNDP-SCs and hBM-MSCs were treated with 5-azacytidine to acquire a myocyte phenotype in culture. Within 8 days following seeding, the first myoblasts fused to form small myotubes. These immature myotubes were thin and short with centrally located, clustered nuclei that differentiated during the next 2–3 days into large multinucleate syncytia (Fig. 10D-a–c). The myogenic cells were strongly positive for all myogenic lineage markers (Fig. 9D-b-c). Data for hBM-MSCs are not shown.

#### Neurogenic differentiation

Neuron-like cells derived from hNDP-SCs displayed distinct morphologies, ranging from extensively simply bipolar to large, branched multipolar cells (Fig. 10E-a–c). Within 24 h of exposure to neurogenic differentiation induction medium, changes in the morphology of some of the SCs were apparent (Fig. 10E-a). To characterise neuronal identity further, differentiated SCs were stained for



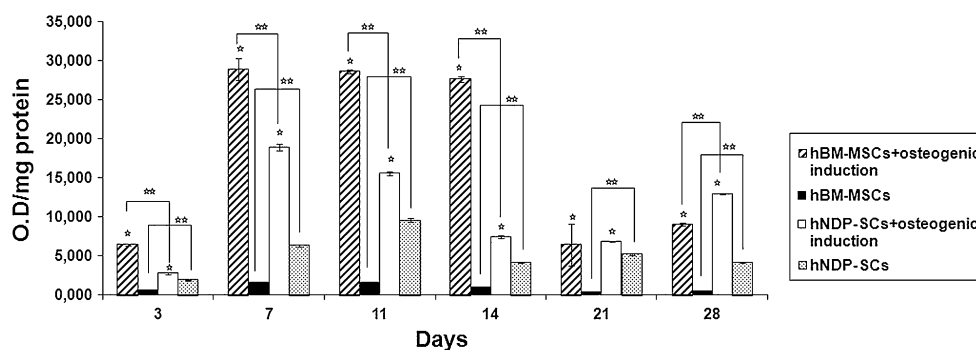


**Fig. 11** The alkaline phosphatase activity was expressed in terms of the mol *p*-nitrophenol/min/mg protein. The protein content was determined using a protein assay kit (Bio-Rad, Hercules, CA, USA) with

bovine serum albumin as the standard. Data are represented as mean values  $\pm$  standard deviation

neuron or glial cell specific markers including GFAP (Fig. 10E-b), *c-fos* (Fig. 10E-b), beta-III tubulin (Fig. 10E-c), beta-tubulin (Fig. 10E-c),  $\gamma$ -enolase, neurofilament, MAP2a,b and nestin (data not shown). During differentiation, it was realised that in addition to the morphological changes, which causes the cells to appear neuron-glial-like, the immunohistochemical staining intensities for all neuronal markers increased. This finding may be due to cytoplasm shrinkage, which causes an intense staining pattern. Alternatively, an increase in nuclear staining plus the cytoplasmic staining suggests otherwise. Therefore, we think that the apparent increase, especially in *c-fos* expression, was indicative of high cellular activity towards differentiation (Fig. 10E-b).

## Discussion

Gronthos et al. (2000) identified a population of human dental pulp stem cells (DP-SCs) that can develop into odontoblasts, the cells that form the mineralised matrix of dentin. DP-SCs display similar features to bone marrow-derived MSCs. For example, both cell types adhere to plastic and form colonies. In later studies, researchers obtained two different cell types similar to stem cells or stem cell-like cells. The first group of cells do not exhibit expression of hematopoietic markers (CD34, CD45 and CD14) but express MSC specific markers (STRO-1, CD29, CD44 and CD13) (Gronthos et al. 2000, 2002; Miura et al. 2003; Kerkis et al. 2006; Jo et al. 2007). The other group of cells are composed of *c-kit*<sup>+</sup>/*CD34*<sup>+</sup>/*CD45*<sup>-</sup> cells and undergo osteogenic differentiation both in vivo and in vitro (Laino et al. 2005; d'Aquino et al. 2007). Our data indicated that hNDP-SCs expressed CD13, CD44, CD73, CD90, CD146 and CD166, but not CD3, CD8, CD10, CD11b, CD14, CD15, CD19, CD33, CD34, CD45, CD71, CD117, and HLA-DR and could be classified within the first group of cells mentioned above. The hNDP-SCs studied here exhibited a

higher proliferation rate compared to hBM-MSCs in vitro. This finding may be attributed to the source of the hNDP-SCs: cells from NDP may have embryonic/foetal cell characteristics and are, therefore, prone to proliferation.

Cellular characteristics of hNDP-SCs, as determined by transmission electron microscopy, depicted more developed and metabolically active cells. The presence of rER stacks, closely packed cristae containing mitochondria and large peripheral collections of unbound glycogen are major features of hNDP-SCs.

In this study, hNDP-SCs and hBM-MSCs not induced to differentiate expressed antigens that are indicators of glial and neuronal ( $\gamma$ -enolase, MAP2a,b,  $\beta$ III tubulin, and GFAP), myogenic (myogenin, myosinIIa, desmin, actin and  $\alpha$ -SMA), osteogenic (osteonectin, osteocalcin, osteopontin, type I collagen, BMP-2 and BMP-4) and chondrogenic (type II collagen) differentiation as demonstrated by immunohistochemical staining. To our knowledge, these data are the first that report expression of these markers in hNDP-SCs and hBM-MSCs.

In addition, we have demonstrated that hNDP-SCs and hBM-MSCs expressed osteogenic, chondrogenic, adipogenic, myogenic and neurogenic markers under basal conditions via reverse transcriptase-PCR and have the capacity to differentiate into mature adipocytes, myoblasts, neuroglial cells, chondroblasts and osteoblasts in vitro under permissive differentiation conditions. Therefore, it may be stated that MSCs have diverse immunophenotypic characteristics. This finding may explain why they easily differentiate into adipose, bone, cartilage, muscle and neural cells. In addition, the expression of oct-4, Rex-1, Nanog, FoxD3 and Sox2 may reflect a propensity for pluripotency. Therefore, it was not surprising to observe that the cells expressed mesoderm and ectoderm precursor markers.

Telomerase activity of hNDP-SCs at different passages was reduced at higher population doublings. This result was in accordance with the results in the literature that showed telomerase activity among MSCs was highest at the



early passages and varies between cell types (Izadpanah et al. 2006). Telomerase activity was not detected the hBM-MSCs, which supports previous findings in the literature that stated no telomerase activity could be detected even using sensitive assays (Sonoyama et al. 2006; Serakinci et al. 2008). This finding suggests that to some extent, hBM-MSCs may use other mechanisms for telomere maintenance, such as alternative lengthening (ALT pathway). In this study, it was found that hNDP-MSCs showed a greater proliferation capacity than hBM-MSCs, which may be explained by the moderate telomerase activity of hBM-MSCs.

We studied the potential of hNDP-SCs to differentiate into adipocytes, osteoblasts, chondroblasts, myoblasts and neuro-glial cells of at least two germ layers in comparison to hBM-MSCs. ALP serves as a useful marker for the transition from the proliferative period to matrix maturation in osteogenesis. In our study, a time-dependent effect of osteogenic medium on ALP activity was observed in both cell lines. ALP activity increased in the control cells and in the cells induced for osteogenic differentiation after 3 days of culturing. ALP activity increased approximately fivefold after 1 week of culturing and continued to increase. After 14 days of culturing, the activity stopped rising and started to decrease. These results are supported by the findings of previous studies (Myginda et al. 2007; Bjerre et al. 2008). The ALP levels of hBM-MSCs were higher than the levels in hNDP-SCs. Cells from hNDP exhibited a low but increasing level of ALP activity; however, did not differentiate. This result may indicate their intrinsic tendency of differentiation towards odontoblasts. However, clonally selected cells still need to be tested to confirm this result.

In conclusion, this report described the first successful isolation and characterisation of hNDP-SCs. Although small variations were observed in the cells that most likely reflect a specialised gene program related to their anatomical localisation, there were no significant differences in comparison to other hBM-MSCs.

**Acknowledgment** We thank Özlem Sağlam and Gülay Bayazit for her excellent technical assistance.

## References

- Arthur A, Rychkov G, Shi S, Koblar SA, Gronthos S (2008) Adult human dental pulp stem cells differentiate toward functionally active neurons under appropriate environmental cues. *Stem Cells* 26:1787–1795
- Bjerre L, Bunger CE, Kassem M, Mygind T (2008) Flow perfusion culture of human mesenchymal stem cells on silicate-substituted tricalcium phosphate scaffolds. *Biomaterials* 29:2616–2627
- d'Aquino R, Graziano A, Sampaolesi M, Laino G, Pirozzi G, De Rosa A, Papaccio G (2007) Human postnatal dental pulp cells co-differentiate into osteoblasts and endothelial cells: a pivotal synergy leading to adult bone tissue formation. *Cell Death Differ* 14:1162–1171
- Gandia C, Armiñan A, García-Verdugo JM et al (2008) Human dental pulp stem cells improve left ventricular function, induce angiogenesis, and reduce infarct size in rats with acute myocardial infarction. *Stem Cells* 26:638–645
- Gronthos S, Mankani M, Brahimi J, Robey PG, Shi S (2000) Postnatal human dental pulp stem cells (DPSCs) in vitro and in vivo. *Proc Natl Acad Sci USA* 97:13625–13630
- Gronthos S, Brahimi J, Li W, Fisher LW, Cherman N, Boyde A, DenBesten P, Robey PG, Shi S (2002) Stem cell properties of human dental pulp stem cells. *J Dent Res* 81:531–535
- Huang AH, Chen YK, Lin LM, Shieh TY, Chan AW (2008) Isolation and characterization of dental pulp stem cells from a supernumerary tooth. *J Oral Pathol Med* 37:571–574
- Ikeda E, Hirose M, Kotobuki N, Shimaoka H, Tadokoro M, Maeda M, Hayashi Y, Kirita T, Ohgushi H (2006) Osteogenic differentiation of human dental papilla mesenchymal cells. *Biochem Biophys Res Commun* 342:1257–1262
- Iohara K, Nakashima M, Ito M, Ishikawa M, Nakasima A, Akamine A (2004) Dentin regeneration by dental pulp stem cell therapy with recombinant human bone morphogenetic protein 2. *J Dent Res* 83:590–595
- Izadpanah R, Trygg C, Patel B, Kriedt C, Dufour J, Gimble JM, Bunnett BA (2006) Biologic properties of mesenchymal stem cells derived from bone marrow and adipose tissue. *J Cell Biochem* 99:1285–1297
- Jo YY, Lee HJ, Kook SY, Choung HW, Park JY, Chung JH, Choung YH, Kim ES, Yang HC, Choung PH (2007) Isolation and characterization of postnatal stem cells from human dental tissues. *Tissue Eng* 13:767–773
- Kerkis I, Kerkis A, Dozortsev D, Stukart-Parsons GC, Gomes Massironi SM, Pereira LV, Caplan AI, Cerruti HF (2006) Isolation and characterization of a population of immature dental pulp stem cells expressing OCT-4 and other embryonic stem cell markers. *Cells Tissues Organs* 184:105–116
- Laino G, d'Aquino R, Graziano A, Lanza V, Carinci F, Naro F, Pirozzi G, Papaccio G (2005) A new population of human adult dental pulp stem cells: a useful source of living autologous fibrous bone tissue (LAB). *J Bone Miner Res* 20:1394–1402
- Miura M, Gronthos S, Zhao M, Lu B, Fisher LW, Robey PG, Shi S (2003) SHED: stem cells from human exfoliated deciduous teeth. *Proc Natl Acad Sci USA* 100:5807–5812
- Myginda T, Stiehler M, Baatrup A, Li H, Zou X, Flyvbjerg A, Kassem M, Bünger C (2007) Mesenchymal stem cell ingrowth and differentiation on coralline hydroxyapatite scaffolds. *Biomaterials* 28:1036–1047
- Nosrat IV, Widenfalk J, Olson L, Nosrat CA (2001) Dental pulp cells produce neurotrophic factors, interact with trigeminal neurons in vitro, and rescue motoneurons after spinal cord injury. *Dev Biol* 238:120–132
- Otaki S, Ueshima S, Shiraishi K, Sugiyama K, Hamada S, Yorimoto M, Matsuo O (2007) Mesenchymal progenitor cells in adult human dental pulp and their ability to form bone when transplanted into immunocompromised mice. *Cell Biol Int* 31:1191–1197
- Papaccio G, Graziano A, d'Aquino R, Graziano MF, Pirozzi G, Menditti D, De Rosa A, Carinci F, Laino G (2006) Long-term cryopreservation of dental pulp stem cells (SBP-DPSCs) and their differentiated osteoblasts: a cell source for tissue repair. *J Cell Physiol* 208:319–325
- Serakinci N, Graakjaer J, Kolvraa S (2008) Telomere stability and telomerase in mesenchymal stem cells. *Biochimie* 90:33–40
- Shi S, Robey PG, Gronthos S (2001) Comparison of human dental pulp and bone marrow stromal stem cells by cDNA microarray analysis. *Bone* 29:532–539
- Sonoyama W, Liu Y, Fang D, Yamaza T, Seo BM, Zhang C, Liu H, Gronthos S, Wang CY, Shi S, Wang S (2006) Mesenchymal stem

- cell-mediated functional tooth regeneration in swine. PLoS ONE. doi:[10.1371/journal.pone.0000079](https://doi.org/10.1371/journal.pone.0000079)
- Struys T, Krage T, Martens W, Theunissen E, Moreels M, Lambrichts I (2007) Metallothionein: a possible new marker for human dental pulp stem cells. *Eur Cells Mater* 14:131
- Wu L, Wu Y, Lin Y, Jing W, Nie X, Qiao J, Liu L, Tang W, Tian W (2007) Osteogenic differentiation of adipose derived stem cells promoted by overexpression of osterix. *Mol Cell Biochem* 301:83–92
- Yu J, Wang Y, Deng Z, Tang L, Li Y, Shi J, Jin Y (2007) Odontogenic capability: bone marrow stromal stem cells versus dental pulp stem cells. *Biol Cell* 99:465–474
- Zhang W, Walboomers XF, Shi S, Fan M, Jansen JA (2006a) Multilineage differentiation potential of stem cells derived from human dental pulp after cryopreservation. *Tissue Eng* 12:2813–2823
- Zhang W, Walboomers XF, van Kuppevelt TH, Daamen WF, Bian Z, Jansen JA (2006b) The performance of human dental pulp stem cells on different three-dimensional scaffold materials. *Biomaterials* 27:5658–5668